Surface & Coatings Technology 347 (2018) 92–98

Contents lists available at ScienceDirect

Surface & Coatings Technology

journal homepage: www.elsevier.com/locate/surfcoat

Influence of coating thickness and substrate on stresses and mechanical properties of (Ti,Al,Ta)N/(Al,Cr)N multilayers

W.M. Seidl[a], M. Bartosik[a,b,*], S. Kolozsvári[c], H. Bolvardi[d], P.H. Mayrhofer[a,b]

[a] Christian Doppler Laboratory for Application Oriented Coating Development, TU Wien, Austria
[b] Institute of Materials Science and Technology, TU Wien, Austria
[c] Plansee Composite Materials GmbH, Germany
[d] Oerlikon Balzers, Oerlikon Surface Solutions AG, Liechtenstein

ARTICLE INFO

Keywords:
Residual stress
Thick coatings
Al-Cr-N
Ti-Al-Ta-N
PVD

ABSTRACT

The build-up of residual stresses in physical vapour deposited hard coatings can lead to delamination and crack formation in thin films when a critical stress value is exceeded, which typically limits the possible coating thickness. Because for some applications rather thick coatings are desired, the stress evolution with coating thickness is of uttermost importance. Therefore, we systematically studied the residual stresses of arc evaporated 0.8, 1.6, 2.4, 4, 8, and 16 µm thick $Al_{0.62}Cr_{0.38}N/Ti_{0.44}Al_{0.41}Ta_{0.15}N$ multilayer coatings (having a bilayer period of 24 nm), grown on monocrystalline Si and Al_2O_3 as well as on polycrystalline hard metal and austenitic stainless steel. Only the thinner coatings exhibit a pronounced stress-thickness dependence, whereas coatings with thicknesses ≥4 µm exhibit similar stresses (within the error of measurement). The measured indentation modulus of the coatings on flexible substrates (Si and austenitic stainless steel) increases to ~490 GPa, but those on stiff substrates (Al_2O_3 and hard metal) decreases to ~490 GPa, with increasing coating thickness to 16 µm. Contrary, the measured hardness of the coatings slightly increases with increasing thickness to 4 µm, and stays constant for thicker coatings, because the substrates are softer than the coating. The hardness values of the thicker coatings (≥4 µm) are 37.3 ± 0.7, 38.2 ± 0.6, 35.8 ± 0.8, and 34.0 ± 1.2 GPa on Si, austenitic stainless steel, Al_2O_3, and hard metal, respectively. Consequently, even the rather thick coatings still show lower hardness values on stiffer substrates.

1. Introduction

Physical vapour deposited $Al_xCr_{1-x}N$ and $Ti_{1-x}Al_xN$ are two of the most universally used hard coating systems since many years. $Al_xCr_{1-x}N$ features some of the best thermo-mechanical properties paired with outstanding high temperature oxidation resistance. $Ti_{1-x}Al_xN$ on the other hand is well-known for its excellent wear resistance and mechanical properties [1–7]. By alloying Ta to $Ti_{1-x}Al_xN$, the high temperature performance can be increased significantly, but still the oxidation resistance is not as good as that of $Al_xCr_{1-x}N$ [5,8]. Combining $Ti_{1-x-y}Al_{x-y}Ta_yN$ and $Al_xCr_{1-x}N$ in a nanolayered architecture led to multilayer coatings, which outperform the monolithically grown constituents in terms of their mechanical properties, while almost maintaining the excellent oxidation resistance of $Al_xCr_{1-x}N$ [9].

Thick coatings of over 15 µm thickness help to maximise the protection of the underlying parts against mechanical and chemical influences [10]. In order to synthesise such thick coatings, however, sophisticated knowledge of the residual stress state in the coatings is necessary [11,12]. One source for the formation of residual stresses in thin films can be related to the different coefficients of thermal expansion (CTE) of substrate and coating. Such thermally induced stresses develop upon cooling down from deposition to room temperature or due to temperature changes arising in application. The CTE of $Ti_{0.45}Al_{0.55}N$ and $Al_{0.31}Cr_{0.69}N$ is about $6.0{\cdot}10^{-6}\,K^{-1}$ and $7.0{\cdot}10^{-6}\,K^{-1}$ at room temperature (RT) [13]. Therefore, we have simply used $6.5{\cdot}10^{-6}\,K^{-1}$ as an approximation for the CTE of our $Al_{0.62}Cr_{0.38}N/Ti_{0.44}Al_{0.41}Ta_{0.15}N$ multilayer coatings.

Depending on the difference in coefficients of thermal expansion between substrate and coating, different behaviours can be observed. If the CTE of coating and substrate is equal, there is no thermally induced stress contribution to the overall residual stresses. On the other hand, if the CTE of the coating is lower than that of the substrate, the thermally induced stresses in the coating upon cooling are compressive. Accordingly, a higher CTE of the coating (with respect to the substrate) leads to thermally induced tensile stresses upon cooling. The thermally induced component of the stresses (within the coating) can easily be

* Corresponding author at: TU Wien, Austria.
E-mail address: matthias.bartosik@tuwien.ac.at (M. Bartosik).

https://doi.org/10.1016/j.surfcoat.2018.04.060
Received 23 December 2017; Received in revised form 19 April 2018; Accepted 20 April 2018
Available online 22 April 2018
0257-8972/

calculated using their elastic modulus and Poisson ratio, the temperature difference, and the difference in coefficient of thermal expansion between substrate and coating [14,15].

Furthermore, the deposition process itself leads to the development of stresses (due to the unavoidable formation of microstructural defects such as point, line, and area defects), often summarised as growth-induced stresses. These strongly depend on the ion bombardment conditions present during the deposition process, because they influence the formation of structural defects. Thus, also the crystallographic texture of the coating plays a huge role. For example, if the texture of the growing film allows for a deeper penetration of the bombarding ions, their energy is distributed over larger regions leading to fewer microstructural defects and thus lower stress values [16]. The residual stresses, especially if they are compressive, lead in many cases to enhanced mechanical properties and are therefore, up to a certain degree, desirable. Too high stresses, on the other hand, can threaten the integrity of the film-substrate composite leading to film delamination or the formation of cracks [17].

Besides thermally and growth induced stresses, a major contribution to the general stress state of the coatings (especially for multilayers and superlattices) are also coherency stresses, for example between adjacent, coherently growing (or partly coherently growing) layers.

Utilising the excellent properties of the $Al_{0.62}Cr_{0.38}N$/$Ti_{0.44}Al_{0.41}Ta_{0.15}N$ multilayer coatings (reported in [9]) for industrial processes, requires the applicability on industrially relevant substrates. In the present work, we thus have chosen W_xC-Co, austenitic stainless steel, Si (100), and Al_2O_3 ($1\bar{1}02$) as substrate materials because they are widely used substrate materials in thin film synthesis. A further important but hardly studied issue is, how the residual stresses in thin films are influenced by the mechanical properties (especially stiffness, yield stress, and ductility) and the CTE of the substrate material itself. Therefore, we have also selected substrate materials with hugely different mechanical properties (Table 1).

2. Experimental

All coatings were arc evaporated using an industrial scale deposition system (Oerlikon Balzers INNOVA), which allows to simultaneously operate six arc sources, which were equipped with four $Ti_{0.45}Al_{0.45}Ta_{0.10}$ and two $Al_{0.70}Cr_{0.30}$ cathodes (prepared by powder metallurgy, Plansee Composite Materials GmbH). The thickness of the multilayer coatings was varied by using different deposition times, while all other parameters were kept constant for all coatings investigated. Chosen deposition durations were 13, 26, 40, 66, 132, and 264 min. The multilayer structure of the coatings was realised through the arrangement of the cathodes in the chamber and double-fold rotation of the substrate holder (see Fig. 1). All coatings were deposited on a wide variety of substrates — polished austenitic stainless steel (1.4571) platelets ($20 \times 7 \times 0.8\,mm^3$), polished monocrystalline Al_2O_3 platelets in ($1\bar{1}02$) orientation ($10 \times 10 \times 0.4\,mm^3$), polished monocrystalline

Table 1
Overview of mechanical properties and CTE for the substrates used [18–22].

	Young's modulus	Yield strength or fracture strength (tension)	Coefficient of thermal expansion at RT
	E	σ	CTE
	GPa	MPa	K^{-1}
Si (100)	130	~700	$\sim 3 \times 10^{-6}$
Al_2O_3	470	2250	$\sim 5 \times 10^{-6}$
W_xC-Co	~500–600	~1500–3000	$5–6 \times 10^{-6}$
Austenitic stainless steel	200	240	$\sim 17 \times 10^{-6}$

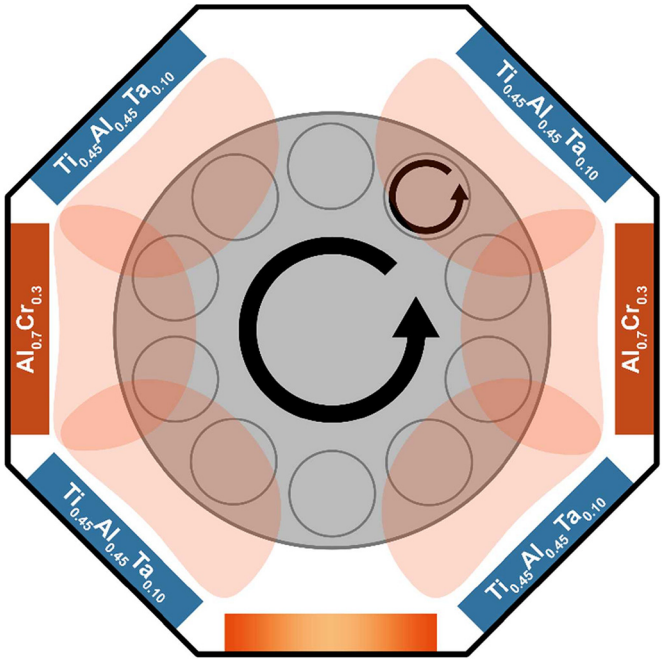

Fig. 1. Schematic arrangement of the cathodes in the deposition chamber and the double-fold rotating carousel for the substrates.

(111) silicon substrates ($20 \times 7 \times 0.38\,mm^3$), and cemented carbide (W_xC-Co) cutting inserts ($12 \times 12 \times 3\,mm^3$). Before mounting the substrates on the carousel, they were cleaned in an ultrasonic bath with ethanol and acetone for 5 min each. The minimum distance between target and substrate holder in the chamber was about 25 cm. The base pressure prior to the deposition was always below $1{\cdot}10^{-4}$ Pa. A deposition temperature (T_{dep}) of 480 °C was achieved with a combined plasma and radiator heating process. The process temperature was measured by two thermocouples. Both were located on the height of the substrate holders, one on the upper and one on the lower end. Prior to the actual deposition, the carousel with the mounted substrates were Ar ion etched for 30 min using the Oerlikon Balzers Central Beam Etching (CBE) technology. The N_2 process gas flow was regulated to a constant pressure of 3.5 Pa ($3.5{\cdot}10^{-2}$ mbar). The arc sources were operated with currents of 150 and 200 A when equipped with $Al_{0.70}Cr_{0.30}$ or $Ti_{0.45}Al_{0.45}Ta_{0.10}$ cathodes, respectively. The substrate bias potential was kept at −40 V for all depositions.

The analysis of the film structures was carried out via X-ray diffraction (XRD) using a PANalytical X'pert Pro MPD diffractometer equipped with a CuK_α radiation source. The diffractometer was adjusted in Bragg-Brentano geometry for all measurements. Cross-section micrographs of the films and film chemistry were obtained with a FEGSEM Quanta F 200 Scanning Electron Microscope (SEM) and an attached Energy-Dispersive X-ray Spectroscopy (EDS) detector with an acceleration voltage of 20 kV, respectively.

Both, indentation hardness (H) and indentation modulus (E), were obtained from nanoindentation curves recorded with an Ultra-Micro-Indentation System (UMIS) equipped with a Berkovich diamond tip. The testing was conducted with steps of 1 mN in a range from 5 to 20 mN. The indentation hardness and modulus values were obtained by evaluating the load-displacement curves using the procedure by Oliver and Pharr [23,24]. According to Bückle [25] we assured an indentation depth of under 10% of the total coating thickness to minimise influence of the substrates underneath.

We analysed the residual stresses of all coatings by applying the $\sin^2\psi$ method [26,27] in a $\sin^2\psi$ range from 0 to 0.8 using $\Delta\sin^2\psi$ steps of 0.1. A Pseudo-Voigt fit function was used to determine the peak positions of the (111) XRD reflections for coatings on austenitic stainless